Pet. Sci. (2017) 14:203–213
DOI 10.1007/s12182-016-0145-y

ORIGINAL PAPER

Green and efficient dry gel conversion synthesis of SAPO-34 catalyst with plate-like morphology

Chun-Yu Di[1] · Xiao-Feng Li[1] · Ping Wang[1] · Zhi-Hong Li[1] · Bin-Bin Fan[1] · Tao Dou[2]

Received: 31 July 2016 / Published online: 30 December 2016

Abstract SAPO-34 catalyst with plate-like morphology was designed and synthesized for the first time, by the dry gel conversion method using cheap triethylamine as a structure-directing agent assisted with seed suspension containing nanosheet-like SAPO-34 seed. The latter played an important role in formation of SAPO-34 (CHA-type) with plate-like morphology. In addition, the yield of the product in the synthesis system containing seed suspension reached 97%, 15% higher than that obtained in the corresponding synthesis system without the seed suspension. Meanwhile, the plate-like SAPO-34 catalysts synthesized by this method exhibited higher selectivity to light olefins and longer lifetime in methanol-to-olefins (MTO) reaction than the traditional cubic SAPO-34 catalyst. This work provides a new technical route for green and efficient synthesis of SAPO-34 catalysts with improved MTO performance.

Keywords SAPO-34 · Dry gel conversion · Green chemistry · Seed suspension · Plate-like · MTO

✉ Bin-Bin Fan
fanbinbin2002@yahoo.com

✉ Tao Dou
dtao1@163.com

[1] College of Chemistry and Chemical Engineering, Taiyuan University of Technology, Taiyuan 030024, Shanxi, China

[2] CNPC Key Laboratory of Catalysis, College of Chemical Engineering, China University of Petroleum, Beijing 102249, China

Edited by Xiu-Qin Zhu

1 Introduction

Ethylene and propylene are the most widely used basic organic chemical materials, and they play an important role in the petrochemical industry. At present, light olefins are mainly produced by cracking light hydrocarbon (naphtha and light diesel oil). However, with the shortage of oil resources, developing alternative routes for ethylene and propylene production has attracted intense attraction, in which the conversion of natural gas or coal to light olefins via methanol is the most promising route (Chen et al. 2005). The conversion process of coal or natural gas to light olefins via methanol is an effective way to solve such problems such as the limited oil resource and increasing olefins demands (Qi et al. 2005), such as UOP/Hydro's methanol-to-olefins (USA) (Chen et al. 2005), syngas via dimethylether to olefins of Dalian Institute of Chemical Physics (China) (Tian et al. 2015) and Lurgi's methanol to propylene (Rothaemel and Holtmann 2002).

Silicoaluminophosphate (SAPO) molecular sieves have been widely studied because of their many technological applications. Among the SAPOs, SAPO-34 with a chabazite-related structure has exhibited excellent catalytic performance in the methanol-to-olefin (MTO) conversion due to its relatively small pore diameter (Pastore et al. 2005), medium acid strength and high hydrothermal stability (Marchi and Froment 1991; Wei et al. 2012; Wilson and Barger 1999). However, SAPO-34 is easily deactivated by coke, which can heavily block the internal channels of the SAPO-34 crystals and decrease both activity and selectivity, resulting in a short catalyst lifetime (Qi et al. 2007; Lee et al. 2007). During the MTO process, coke formation is related to many factors, such as Si/Al ratio (Xu et al. 2008), acidity (Ye et al. 2011), crystal morphology, as well as crystal size (Chen et al. 1999; Álvaro-Muñoz et al. 2012),

in which the catalyst acidity and size are two important factors. Studies on the crystal size and morphology have shown that SAPO-34 catalysts with small crystal size or with nanosheet-like morphology generally exhibit better catalytic activity, selectivity and longer lifetime due to enhancing the accessibility of methanol into its cages and promoting the diffusion of the products. However, work on synthesis of SAPO-34 with nanosheet-like or plate-like morphology is very limited. Recently, Sun et al. (2014) prepared nanosheet-like SAPO-34 and SAPO-18 molecular sieves with different silicon contents under hydrothermal conditions by using tetraethylammonium hydroxide (TEAOH) as the template, and the catalysts showed high catalytic activity in the MTO reaction. However, the employed hydrothermal synthesis method has the following problems: (1) producing large amounts of waste and harmful gas; (2) using expensive TEAOH; and (3) difficulties in solid–liquid separation (Roth et al. 2014; Choi et al. 2009). In order to overcome these problems, a new alternative synthesis method, i.e., zeolites-dry gel conversion (DGC), used in the synthesis of SAPO molecular sieves has recently shown good potential. This method involves treating pre-dried gel powder at elevated temperatures and pressures to form crystalline molecular sieves (Xu et al. 1990; Rao et al. 1998). Compared with the traditional hydrothermal method, DGC does not produce mother liquor (Yang et al. 2012), can avoid complicated separation processes (Yang et al. 2010) and can give high product yield (Matsukata et al. 1999; Cundy and Cox 2003). In addition, DGC uses a lower amount of organic template and the organic template is easy to recycle and reuse. Therefore, DGC is more environmentally friendly and economical. Many kinds of aluminophosphates (AlPO) and silicoaluminophosphates (SAPOs) have been synthesized by dry gel conversion (Askari et al. 2014). For example, Hirota et al. (2010) synthesized SAPO-34 with an average crystal size of 75 nm by DGC, using TEAOH as the structure-directing agent. However, to our best knowledge, nanosized crystalline catalysts often suffer from some problems, such as low product yield, low hydrothermal stability and crystalline defects due to the intergrowth of crystals. Hence, a novel synthesis strategy is desirable for design and synthesis of highly hydrothermal-stable and plate-like SAPO-34 molecular sieve with a high yield by DGC. In addition, SAPO-34 molecular sieves with low silicon content generally have longer lifetime in the MTO reaction due to their low acid strength (Dahl et al. 1999; Izadbakhsh et al. 2009a, b). But reports on synthesis of SAPO-34 molecular sieves with low silicon content by DGC are scarce.

In this work, we developed a seed suspension-assisted method (containing nanosheet-like SAPO-34 seed) for preparation of SAPO-34 molecular sieves with plate-like morphology by DGC (Fig. 1) using cheap triethylamine (TEA) as the structure-directing agent (SDA). The results showed that this novel strategy could synthesize highly hydrothermal-stable and plate-like SAPO-34 molecular sieve product with a low silicon content, and the product yield was up to 97%. Compared with the traditional cubic SAPO-34 molecular sieve, the plate-like SAPO-34 catalysts synthesized by this method exhibited high selectivity to light olefins (ethylene + propylene) and long lifetime in methanol-to-olefins (MTO) reaction. The selectivity to light olefins increased from 81% to 87%, and the catalyst lifetime was more than doubled.

2 Experimental

2.1 Synthesis of SAPO-34

The SAPO-34 seed suspension was prepared by hydrothermal crystallization from a gel with a molar composition of 1 Al_2O_3: 0.9 P_2O_5: 0.3 SiO_2: 1.6 TEAOH: 60 H_2O. The gel was put into a stainless steel autoclave lined with Teflon, and then it was heated at 150 °C for 6 h. The obtained slurry mixture was the seed suspension (denoted as SS), and the seed (denoted as SD) of SAPO-34 molecular sieve can be obtained by separating and drying the solid product in the crystal seed suspension.

The SAPO-34 catalysts were synthesized by DGC (Fig. 1) with triethylamine (TEA) as the SDA. The molar composition of the initial gel was 1.0 Al_2O_3: 2.5 TEA: 0.9 P_2O_5: 0.3 SiO_2: 60 H_2O. Different mass percentages of SS were added into the initial gel. The detailed synthesis procedures were as follows. At first, pseudoboehmite (73 wt% Al_2O_3), TEA (Alfa Aesar), silica sol (40 wt% SiO_2) and distilled water were mixed and stirred at room

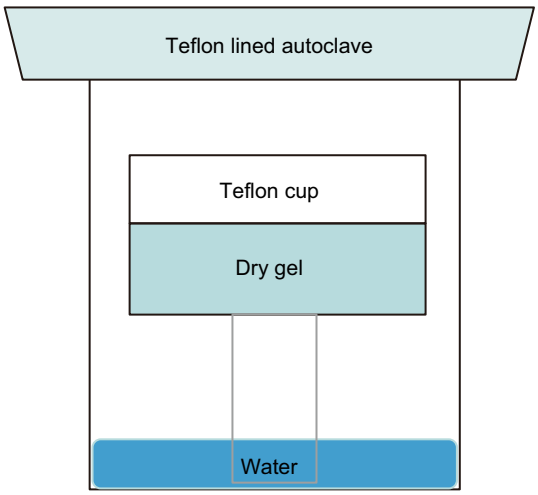

Fig. 1 Diagram of the reaction vessel used in the DGC method

temperature. Then, SS was added to the mixture and stirred. Finally, phosphoric acid (85 wt% H_3PO_4) was added dropwise to the mixture under stirring. The synthesis mixture was stirred and then dried at 110 °C to obtain a dry gel. The dry gel with different amounts of SS was placed in an autoclave, and crystallization was performed at 170 °C for 48 h.

The solid product was washed only once by centrifuging with distilled water and then dried at 100 °C over night. The as-synthesized products were calcined at 550 °C for 5 h to remove the template. The synthesis conditions of different samples are given in Table 1.

2.2 Characterization

The powder X-ray diffraction (XRD) patterns of as-synthesized samples were obtained on a Rigaku D/max-3C X-ray diffractometer (Rigaku Co., Japan) with Cu Kα radiation at 36 kV and 40 mA. The patterns were recorded from 5° to 35° with a step size of 0.02°. N_2 adsorption–desorption was performed at −196 °C using a Quantachrome AUTOSORB-1C instrument (Quantachrome Co., USA). Before the measurement, the samples were vacuum degassed at 300 °C for at least 10 h. The specific surface area (S_{BET}) and the micropore volume were calculated according to Brunauer–Emmett–Teller (BET) equation and t-plot method, respectively. Scanning electron microscope (SEM) images were recorded on a HITACHI S-570 scanning electron microscope. Each sample had been placed onto a carbon membrane, and an Au sputter coating was applied to reduce charging effects. The temperature-programmed desorption of ammonia (NH_3-TPD) was performed on a Micromeritics ASAP 2020C instrument. The sample (0.1 g) was pretreated at 450 °C for 2 h in an Ar flow of 20 mL min^{-1}. After cooling to 100 °C, the sample was saturated with 10 vol% NH_3/Ar, and then the sample was purged with Ar for 1 h to eliminate physically absorbed NH_3. Desorption of NH_3 was carried out from 100 to 600 °C at a heating rate of 5 °C min^{-1}. ^{29}Si MAS NMR spectra were recorded in 7 mm ZrO_2 rotors at 79.5 MHz on a Varian Infinity-plus 400 WB spectrometer, fitted with a BBO (broadband observe) probe. The spinning rate of the samples at the magic angle was 4 kHz. The internal standard for chemical shifts was 2,2-dimethyl-2-silapentane-5-sulfonate sodium salt (DSS).

Table 1 Synthesis conditions, yield and phase of the synthesized SAPO crystals

Samples	SS[a], wt%	SiO_2/Al_2O_3[b]	Yield, %[c]	Phase identity
S-1	0	0.3	82	CHA-type
S-2	10	0.3	88	CHA-type
S-3	20	0.3	97	CHA-type
S-4	30	0.3	91	CHA-type

[a] SS content in the synthesis suspension

[b] SiO_2/Al_2O_3 in dry gel

[c] Product yield calculated by the mass ratio of calcined solid product to SiO_2, Al_2O_3 and P_2O_5 in the synthesis gel

2.3 Catalytic performance

Catalytic activity measurements were carried out in a quartz tubular fixed-bed reactor. First, the catalysts were pressed, crushed and sieved to obtain particle sizes between 250 and 500 μm. Second, 1.0 g of the shaped catalyst was placed into a quartz tube (inner diameter 10 mm) between two quartz-wool plugs. Prior to reaction, the catalyst was activated at 550 °C in air (30 mL min^{-1}) for 2 h. Aqueous methanol solution (95 wt%) was fed into the reactor under atmospheric pressure. The volume hourly space velocity (volume of methanol aqueous solution flowing through a unit volume of catalyst in a unit time) was 3 h^{-1}, and the reaction temperature was 450 °C. The analysis of the reaction products was performed using an on-line gas chromatograph Agilent GC (6890 N), equipped with a flame ionization detector (FID) and Plot-Q column. The conversion and selectivity were calculated on CH_2 basis, and dimethyl ether (DME) was considered to be a reactant for the calculation.

3 Results and discussion

3.1 Crystalline structure and morphological features of SAPO-34 seed

Figure 2a shows the XRD patterns of the as-synthesized SAPO-34 seed (SD) contained in the seed suspension (SS). From Fig. 2a, it can be seen that the representative diffraction peaks at 9.5°, 13.0°, 16.2°, 20.7°, 26.0° and 31.0° were observed in the XRD pattern of the SD, corresponding to pure SAPO-34 with a CHA-structure (Rao and Matsukata 1996). Furthermore, the peaks of the SD are wider than the other as-synthesized samples, indicating that the crystallite size of SD is smaller (Li et al. 2014). This can be further confirmed by the SEM images. As shown in Fig. 2b, the SD has nanosheet-like morphology with an average particle below 200 nm, indicating that the precursor gel at low temperature and short crystallization time can transform to nanosheet-like crystals. This is in agreement with the results reported in the literature (Lei et al. 2013).

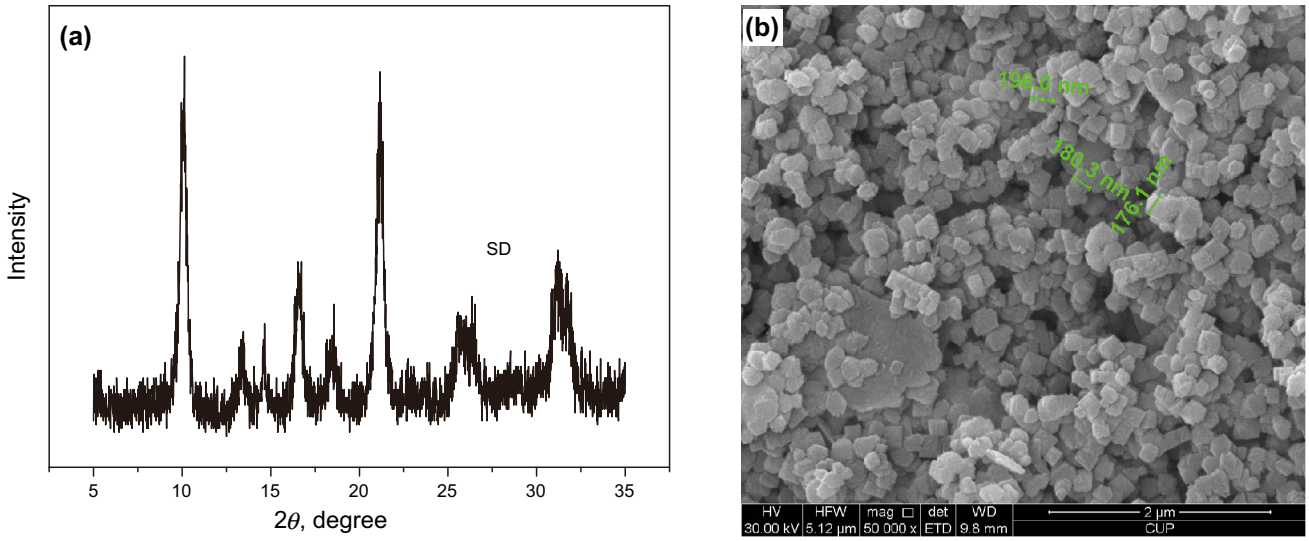

Fig. 2 XRD pattern (**a**) and SEM image (**b**) of the SAPO-34 seed (SD)

3.2 Physicochemical properties of SAPO-34

Figure 3 shows the XRD patterns of the SAPO-34 samples prepared by dry gel conversion with different amounts of SAPO-34 SS. It can be seen that all the synthesized samples showed the typical diffraction patterns of CHA-structure SAPO-34 without the presence of other impurity phases (Lee et al. 2007). However, the SS added into the initial gel influenced the relative intensity of the different diffraction peaks. For S-2, S-3 and S-4 samples, their peak intensities at $2\theta = 20.7°$ were much higher than that of S-1, while their peak intensities at $2\theta = 13.0°$ were much lower than that of S-1. These phenomena indicated that the SS had great influence on the growth of different crystal faces. In addition, as can be seen from Table 1, the SS can significantly improve product yield and promote conversion of more amorphous materials into SAPO-34 molecular sieve. The yield of the sample S-3 was 97%, 15% higher than that of the sample S-1.

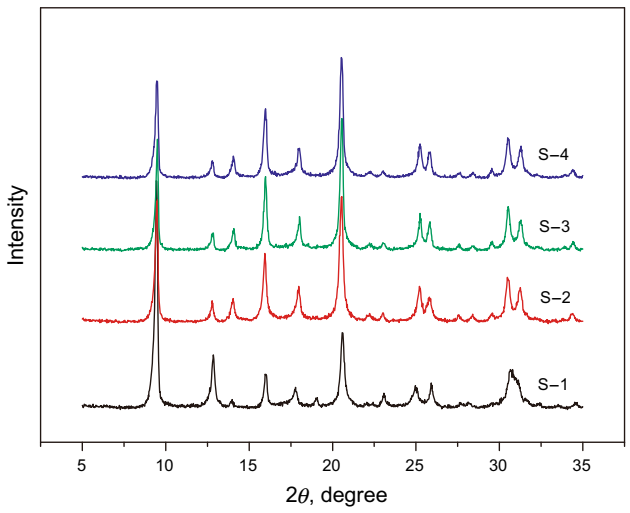

Fig. 3 XRD patterns of the synthesized SAPO-34 samples

Figure 4 shows the SEM images of the different samples. The S-1 sample had a larger cubic crystal structure of about 4 μm, whereas the other synthesized samples exhibited a more plate (or sheet)-like morphology. The reason maybe that seed solution not only provided more crystal nucleus (crystal growth site) but also hindered the growth rate of crystals in one dimension in the dry gel conversion system. Furthermore, with the increase in the amount of SS in the dry gel, the framework of SAPO-34 particles transformed to a plate-like structure with a decrease in thickness, suggesting that the particles mainly grew on the periphery of the nanosheet-like structure of the SD. The thickness of particle S-2 was about 1 μm, while the thickness of particle S-3 was about 500 nm. But when the amount of SS was further increased to 30%, the particles of the obtained S-4 sample became smaller and thinner. Moreover, their plate-like morphologies became very regular. This can be attributed to the addition of the SS to the dry gel. The added SS provided a large number of nucleation sites and the formed silicoaluminophosphate species aggregated into a plate structure.

Based on the XRD and SEM results, we can propose a scheme that qualitatively describes the formation of plate-like SAPO-34 with the assist of seed suspension under the DGC conditions (Fig. 5). The seed suspension contained a large number of very thin SAPO-34 molecular sieve particles. At the same time, there were a large number of SAPO-34 molecular sieve secondary structure units in the seed suspension (Sun et al. 2016). In the dry gel conversion system, the microcrystalline structure guided the surrounding silicon aluminum phosphate species to continue

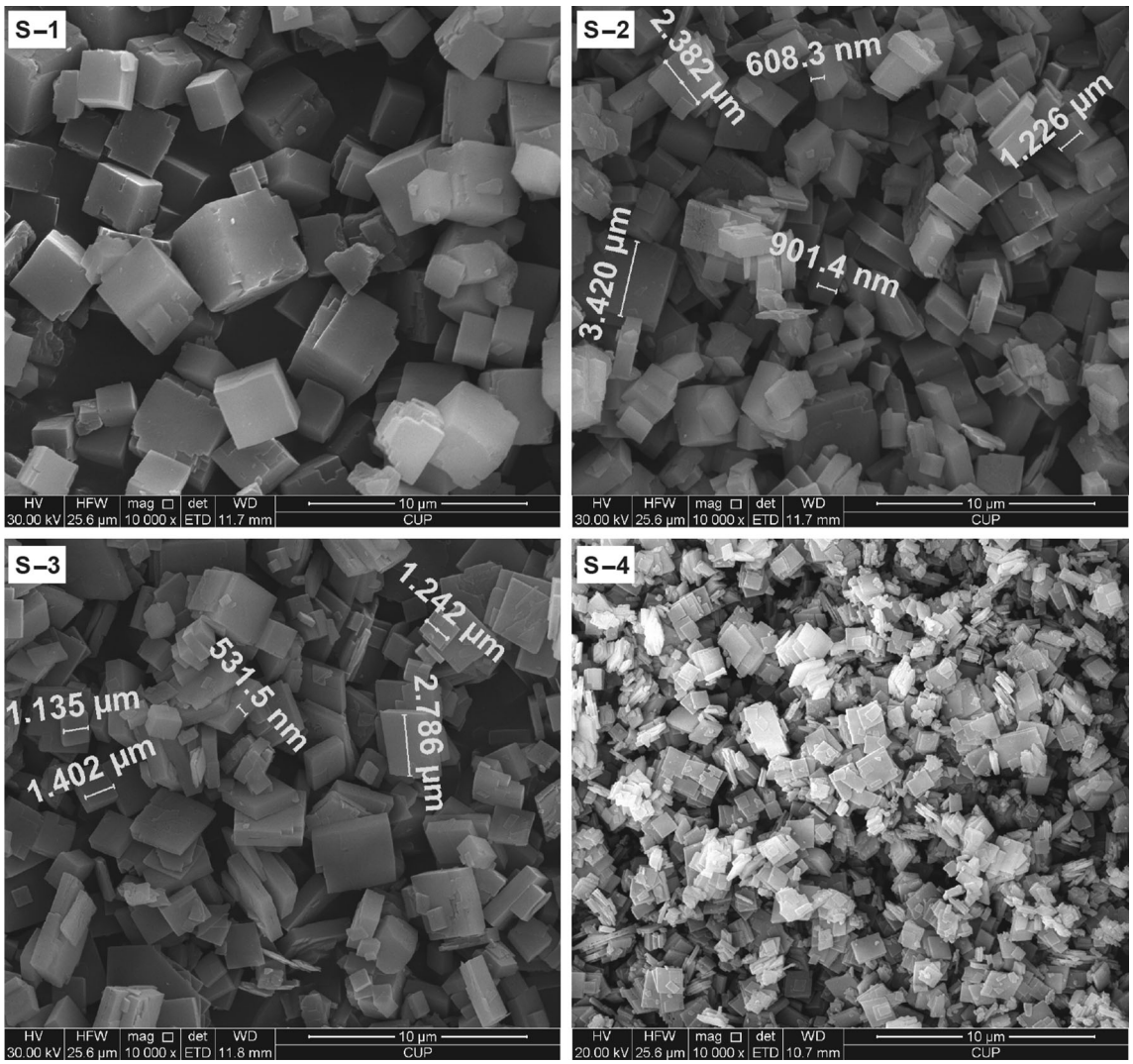

Fig. 4 SEM images of the synthesized SAPO-34 samples

to grow in situ along its edges and eventually form a plate (or sheet-like) SAPO-34 molecular sieve. In addition, Zhang et al. (2011) studied of the crystallization process of the synthesis of SAPO-34 in the dry gel conversion system and found that in the early stage of the crystallization, the gel samples generated a semi-crystalline layered phase. So, they speculate that the layered phase is rich in the double six ring structure, which is very important for the synthesis of SAPO-34 molecular sieve by the dry gel conversion method.

The NH_3-TPD plots of the four catalyst samples are shown in Fig. 6. Four samples gave peaks at approximately 210 and 380 °C, which correspond to the weak and strong acid sites, respectively. The desorption peak at low temperature was attributed to the hydroxyl groups (–OH) bounded to the defect sites, i.e., POH, SiOH and AlOH (Campelo et al. 2000; Dumitriu et al. 1997). As shown in Fig. 6, the four samples had similar acid strength and weak acid amounts, whereas their strong acid amounts slightly decreased with the increase in the added SS.

The nitrogen adsorption–desorption isotherms of four catalyst samples are presented in Fig. 7 with corresponding textural data listed in Table 2. All of the samples had similar micropore volumes in the range of 0.23–0.27 cm^3 g^{-1}, and the samples synthesized using seed suspension exhibited higher BET surface areas.

In the MTO reaction, the catalyst is always used in a harsh high temperature hydrothermal environment. Therefore, it is very necessary to study the hydrothermal stability of different types of catalysts. In this study, four catalyst samples with different morphologies were treated by high temperature hydrothermal aging, and the specific surface area (S_{BET}) was used to reflect their hydrothermal stability. As shown in Fig. 8, the specific surface area (S_{BET}) of the sample S-4 with nanosheet-like structure decreased from 608 to 360 m^2/g after 80 h of hydrothermal aging. In

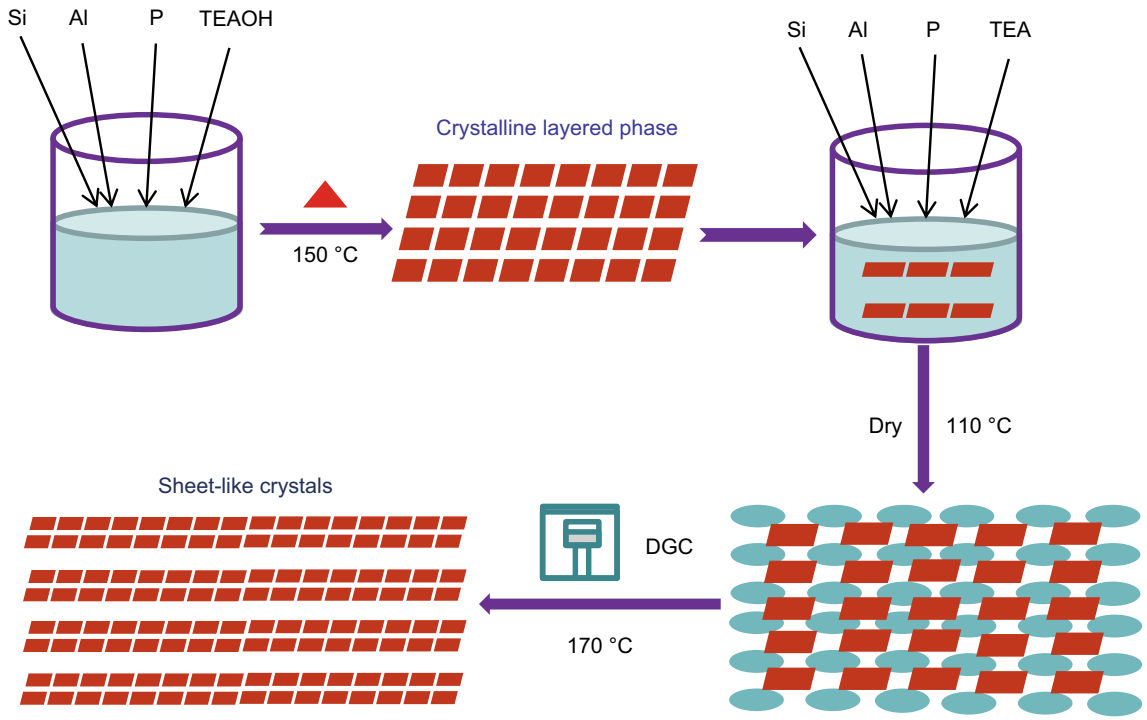

Fig. 5 Illustration of the formation of plate-like SAPO-34 under DGC conditions

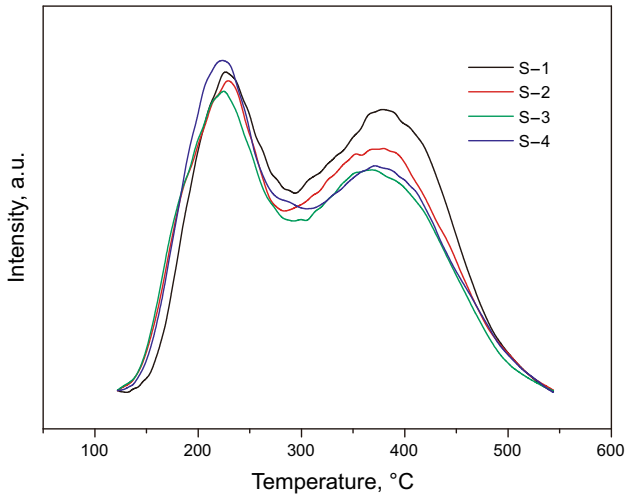

Fig. 6 NH_3-TPD profiles of the synthesized SAPO-34 samples

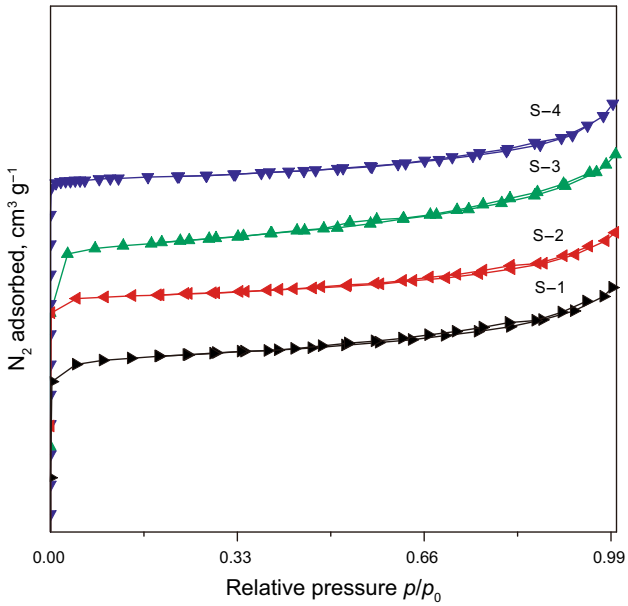

Fig. 7 Nitrogen adsorption–desorption isotherms of the synthesized SAPO-34 samples

contrast, the specific surface areas of cubic or plate-like SAPO-34 molecular sieve samples decreased slightly after the same treatment. These results demonstrated that cubic (S-1) or plate-like SAPO-34 samples (S-2 and S-3) had better hydrothermal stability than the nanosheet-like S-4.

3.3 Catalytic performance

As shown in Fig. 9, SAPO-34 samples synthesized at different conditions showed different methanol conversions and lifetimes. It can be seen that methanol was completely converted over all the catalysts with ethylene and propylene as the main products. Herein, catalyst lifetime is defined as the time when the methanol conversion reaches 98%, and the highest selectivity to light olefins (ethylene and propylene) in the catalyst lifetime is used to represent

Table 2 Physical properties of the synthesized SAPO-34 samples

Samples	Surface area, m^2/g		Micro pore volume, cm^3/g	Particle size, μm
	S_{BET}	$S_{External}$		
S-1	530	8	0.23	4.0
S-2	586	14	0.27	3.0
S-3	612	20	0.28	1.5
S-4	608	22	0.25	1.5

Table 3 MTO reaction results over SAPO-34 samples

Sample	Lifetime, min	Selectivity to product, %								Selectivity to $C_2^=+C_3^=$, %
		CH_4	C_2H_4	C_2H_6	C_3H_6	C_3H_8	C_4	C_5	C_6+	
S-1	80	1.6	40.9	0.5	40.1	1.9	12.4	2.3	0.3	81.0
S-2	120	1.2	44.0	0.3	39.8	0.8	11.5	2.0	0.4	83.8
S-3	180	0.8	45.6	0.3	41.7	0.3	9.7	1.5	0.2	87.2
S-4	150	1.0	45.1	0.3	41.4	0.6	9.1	1.9	0.6	86.6

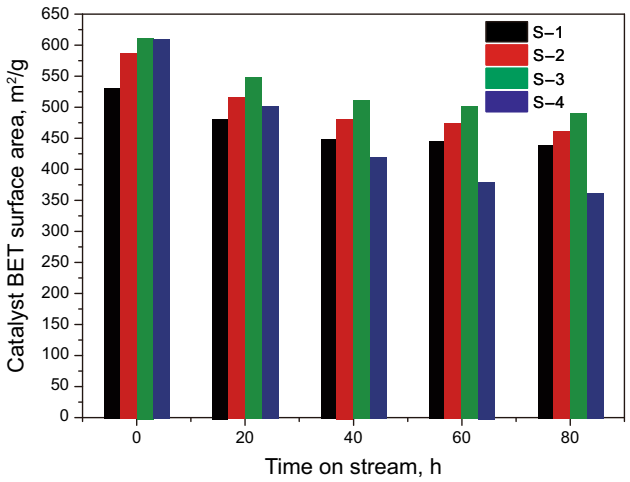

Fig. 8 Duration of hydrothermal aging at 800 °C and 100% steam

the catalytic activity according to the literature (Zhu et al. 2010). Figure 9 and Table 3 show that under the same reaction conditions, the lifetime of sample S-1 was about 80 min with 81% selectivity to ethylene and propylene, whereas the lifetime of S-3 sample with the thinner layers and the largest surface area could reach 180 min with 87% selectivity to ethylene and propylene. The significant improvement of catalyst lifetime and activity attributed to the morphology of the SAPO-34 samples. In MTO reaction, the successive polymerization, which would result in coke formation, may be partly avoided over plate-like SAPO-34 catalysts due to their short diffusion length. The fast deactivation of the S-1 catalyst (conventional large cubic morphology) can be attributed to the coke formation that occurs near the external surface of the catalyst

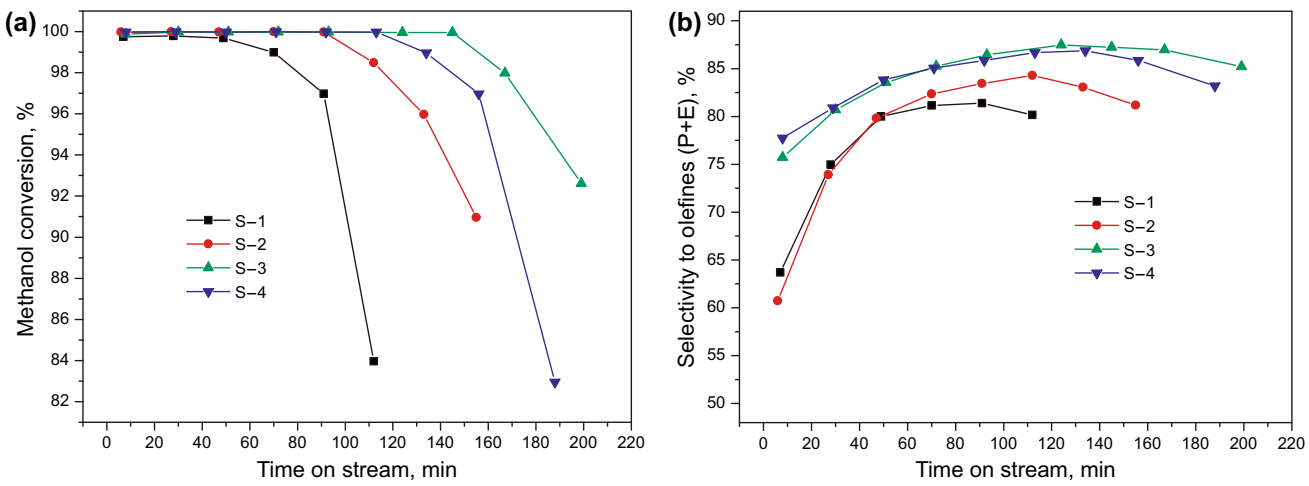

Fig. 9 Catalytic performance of SAPO-34 samples in MTO reaction at 450 °C and 3.0 h^{-1}

Table 4 Synthesis conditions, yield and phase of the synthesized SAPO samples

Samples	SS, wt%	SiO_2/Al_2O_3	Yield, %	Phase identity
S-3	20	0.3	97	CHA-type
S-5	20	0.2	95	CHA-type
S-6	20	0.1	94	CHA-type
S-7	20	0.05	85	CHA-type/AEI-type
S-8	0	0.1	76	CHA-type/AEI-type

particles, gradually blocking the diffusion path of oxygenates to the inner core of catalysts. However, for S-4 catalyst with the thinnest sheet, its deactivation can partially attribute to its poor hydrothermal stability, which could cause its crystal structure destruction under the MTO reaction conditions.

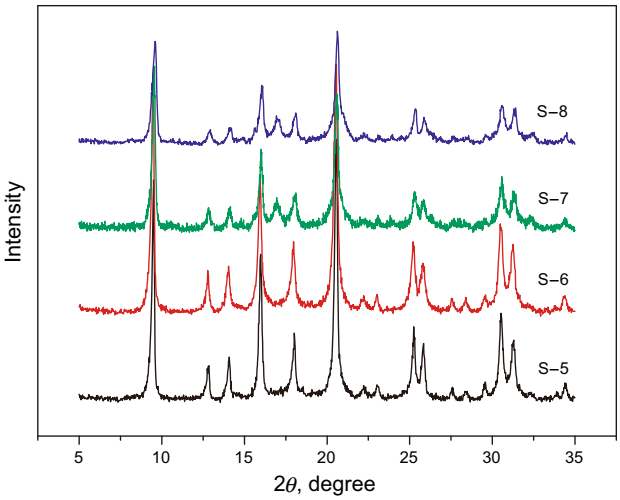

Fig. 10 XRD patterns of the synthesized SAPO-34 samples

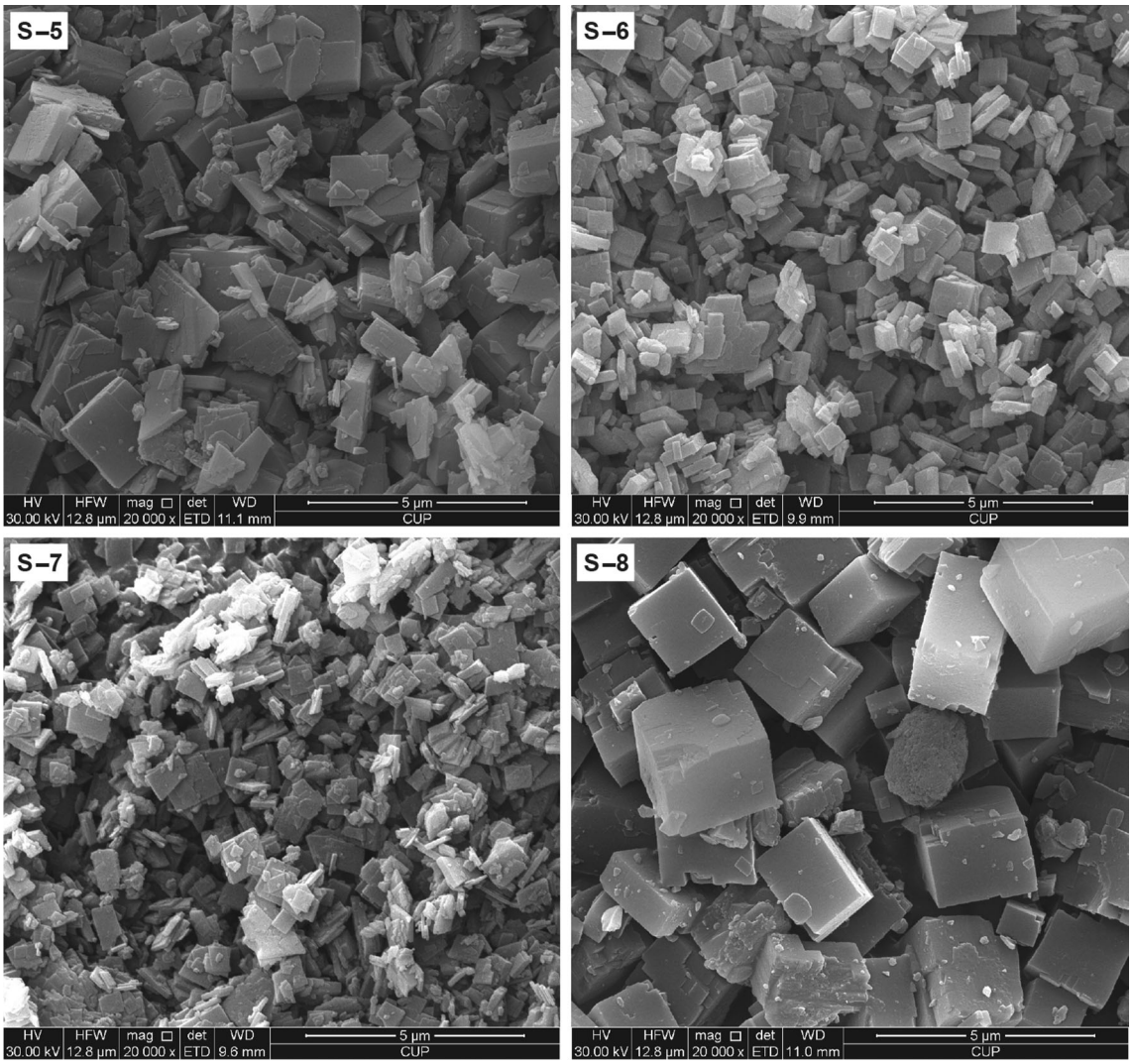

Fig. 11 SEM images of the synthesized SAPO-34 samples

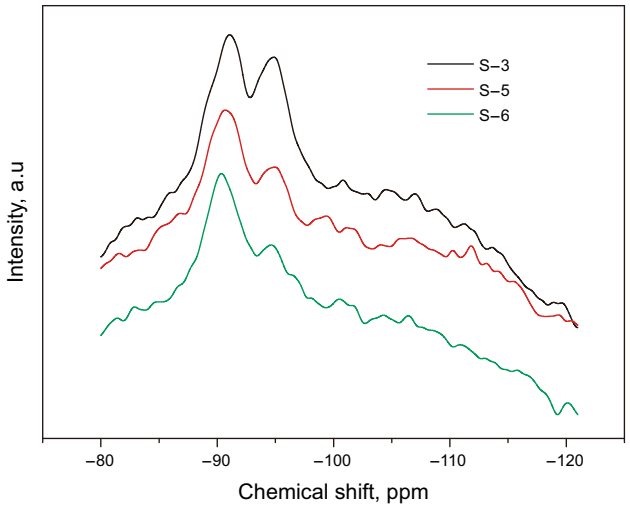

Fig. 12 ^{29}Si MAS NMR spectra of prepared SAPO-34 samples

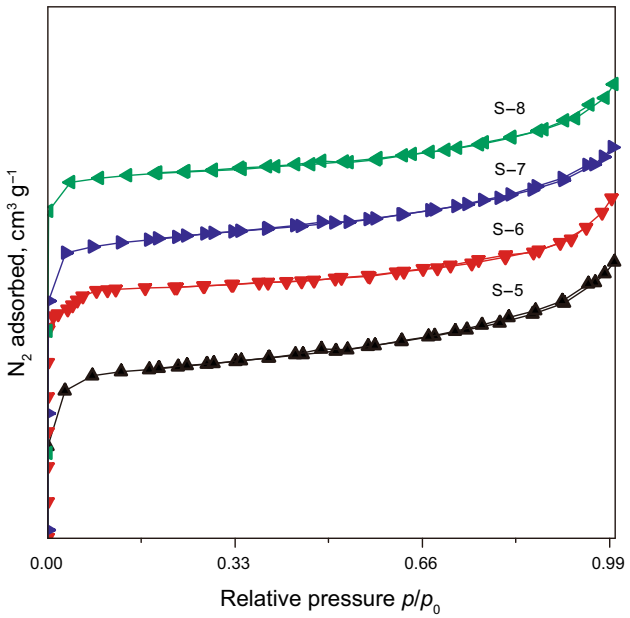

Fig. 13 Nitrogen adsorption–desorption isotherms of the synthesized SAPO-34 samples

3.4 Physicochemical properties of SAPO-34 with low silicon content

Apart from the morphology of SAPO-34 catalyst, the SiO_2/Al_2O_3 ratio of it is also an important factor for the catalytic lifetime (Sastre et al. 1997; Izadbakhsh et al. 2009a, b; Tan et al. 2002). In order to further improve the catalytic performance of SAPO-34 catalyst in MTO reaction, a series of plate-like SAPO-34 molecular sieve with low SiO_2/Al_2O_3 ratio were synthesized by DGC (Table 4).

Samples S-5, S-6 and S-7 were synthesized by DGC with the same compositions as S-3 except for silicon content. The XRD patterns (Fig. 10) of S-5 and S-6 were in agreement with that simulated from the CHA framework type (pure SAPO-34), whereas a small amount of the framework type of AEI was observed in the XRD patterns of S-7 and S-8 (Simmen et al. 1991), indicating that addition of seed suspension (SS) is beneficial to the synthesis of SAPO-34 with low Si contents by DGC.

The SEM images (Fig. 11) showed that S-5, S-6 and S-7 samples exhibited uniform plate-like morphology with the thickness of each plate in the range of 400-500 nm, whereas S-8 synthesized in the absence of the SS showed conventional cube-like morphology with a particle size of about 4 μm.

As shown in Fig. 12, all of the samples showed two major resonances at around −91 and −95 ppm, which were assigned to Si (4Al) and Si (3Al), respectively. The peaks at around −100, −105 and −109 ppm correspond to the signal of Si (2Al), Si (1Al) and Si (0Al), respectively (Shen et al. 2012). Based on the integrated areas of the resonance at −95 ppm, the concentration of Si (4Al) species in the three samples had the following order: S-6 > S-5 > S-3. It seems that under the DGC conditions, the Si species existing in the samples were incorporated into the frameworks via both SM2 (one Si substitution for one P, which forms Si (4Al) species) and SM3 [double Si substitution for pairs of Al and P, which forms Si (nAl) (n = 0–3) species] substitution mechanisms (Tian et al. 2013). Decreasing the Si content in the dry gel can efficiently promote the formation of the Si (4Al) unit. The

Table 5 Physical properties of the synthesized SAPO-34 samples

Samples	Surface area, m^2/g		Micro pore volume, cm^3/g	Particle size, μm
	S_{BET}	$S_{External}$		
S-5	610	19	0.26	1.7
S-6	636	23	0.28	1.2
S-7	536	20	0.23	1.4
S-8	508	9	0.21	3.5

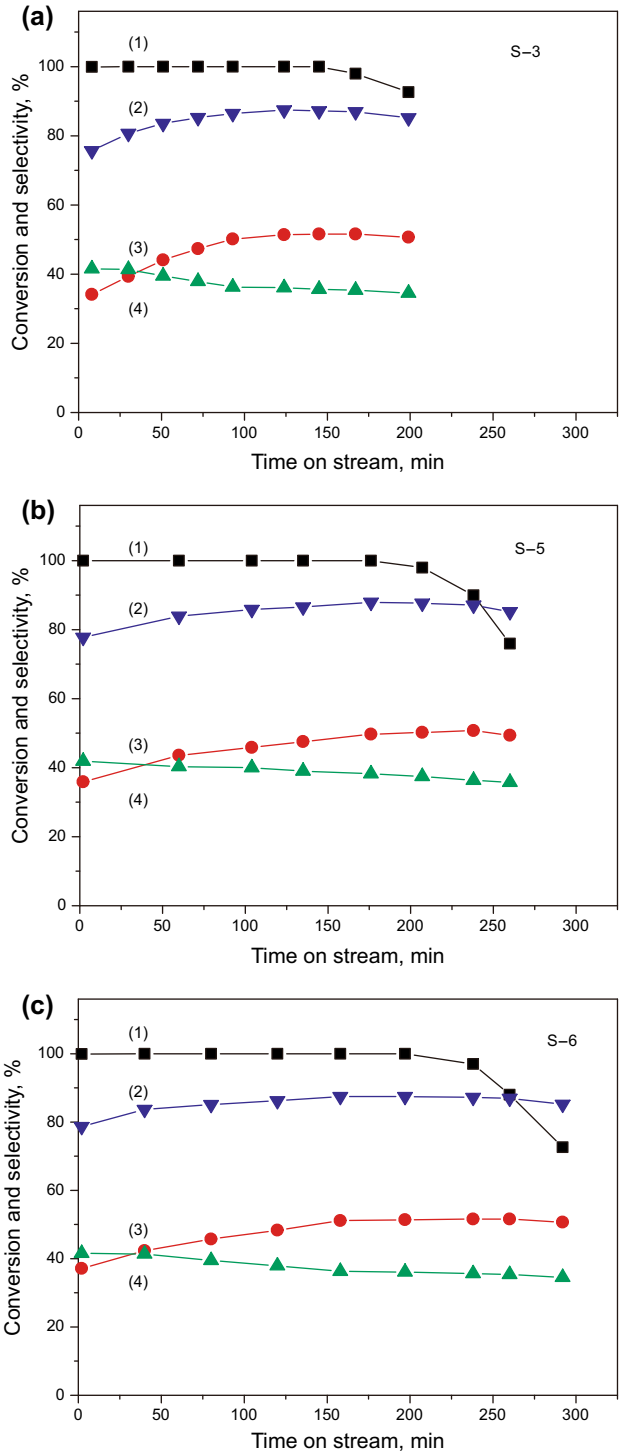

Fig. 14 Performance of SAPO-34 samples in MTO reaction at 450 °C and 3.0 h^{-1} (*1*) Methanol conversion (*black filled squares*), (*2*) selectivity to C_2H_4 and C_3H_6 (*blue filled triangles*), (*3*) selectivity to C_2H_4 (*green filled triangles*), (*4*) selectivity to C_3H_6 (*red filled circles*)

textual properties of the SAPO-34 samples determined with N_2 adsorption–desorption measurement are shown in Fig. 13 and summarized in Table 5. All the isotherms displayed the characteristic type I isotherms, confirming the microporosity of the samples. The BET surface area of S-5 and S-6 was 610 and 636 m^2/g, respectively.

3.5 Catalytic performance of plate-like SAPO-34 with low silicon contents

As shown in Fig. 14, all the catalysts exhibited a long catalyst lifetime and high selectivity to ethylene and propylene because the plate-like crystals can greatly enhance the mass transfer of reactant and generated products during MTO process. Significantly, the S-6 sample synthesized with SiO_2/Al_2O_3 of 0.1 and the highest Si (4Al) content (reducing the acidity of SAPO-34 catalysts) can retain more coke species than the others without fast deactivation (Izadbakhsh et al. 2009a, b). At the same time, for the S-6 sample, the selectivity to ethylene and propylene increased slightly faster than others, indicating that its acidity is more suitable for MTO reaction than others.

4 Conclusion

This work provides a new technical route of green and efficient synthetic strategies to create SAPO-34 molecular sieve with plate-like morphology. SAPO-34 was synthesized by the dry gel conversion method using cheap triethylamine (TEA) as structure-directing agent with the assistance of seed suspension containing nanosheet-like SAPO-34 seed. In addition, the yield of the product in the synthesis system containing seed suspension reached 97%, 15% higher than that obtained in the corresponding synthesis system without the seed suspension. Compared with the traditional cubic SAPO-34 molecular sieve, the selectivity for olefins (ethylene + propylene) for the plate-like SAPO-34 reached 87%, and the catalyst lifetime was more than doubled.

References

Álvaro-Muñoz T, Márquez-Álvarez C, Sastre E. Use of different templates on SAPO-34 synthesis: effect on the acidity and catalytic activity in the MTO reaction. Catal Today. 2012;179(1):27–34. doi:10.1016/j.cattod.2011.07.038.

Askari S, Sedighi Z, Halladj R. Rapid synthesis of SAPO-34 nanocatalyst by dry gel conversion method templated with morphline: investigating the effects of experimental parameters. Microporous Mesoporous Mater. 2014;197(10):229–36. doi:10.1016/j.micromeso.2014.06.028.

Campelo JM, Lafont F, Marinas JM, et al. Studies of catalyst deactivation in methanol conversion with high, medium and small pore silicoaluminophosphates. Appl Catal A Gen. 2000;192(1):85–96. doi:10.1016/S0926-860X(99)00329-4.

Chen JQ, Bozzano A, Glover B, et al. Recent advancements in ethylene and propylene production using the UOP/Hydro MTO process. Catal Today. 2005;106(1–4):103–7. doi:10.1016/j.cattod.2005.07.178.

Chen D, Moljord K, Fuglerud T, et al. The effect of crystal size of SAPO-34 on the selectivity and deactivation of the MTO reaction. Microporous Mesoporous Mater. 1999;29(1–2): 191–203. doi:10.1016/S1387-1811(98)00331-X.

Choi M, Na K, Kim J, et al. ChemInform abstract: stable single-unit-cell nanosheets of zeolite MFI as active and long-lived catalysts. Nature. 2009;461(7261):246–9. doi:10.1038/nature08288.

Cundy CS, Cox PA. The hydrothermal synthesis of zeolites: history and development from the earliest days to the present time. Chem Rev. 2003;103(3):663–702. doi:10.1002/chin.200319217.

Dahl IM, Mostad H, Akporiaye D, et al. Structural and chemical influences on the MTO reaction: a comparison of chabazite and SAPO-34 as MTO catalysts. Microporous Mesoporous Mater. 1999;29(1):185–90. doi:10.1016/S1387-1811(98)00330-8.

Dumitriu E, Azzouz A, Hulea V, et al. Synthesis, characterization and catalytic activity of SAPO-34 obtained with piperidine as templating agent. Microporous Mater. 1997;10(1–3):1–12. doi:10.1016/S0927-6513(96)00107-1.

Hirota Y, Murata K, Tanaka S, et al. Dry gel conversion synthesis of SAPO-34 nanocrystals. Mater Chem Phys. 2010;123(2–3): 507–9. doi:10.1016/j.matchemphys.2010.05.005.

Izadbakhsh A, Farhadi F, Khorasheh F, et al. Effect of SAPO-34's composition on its physico-chemical properties and deactivation in MTO process. Appl Catal A Gen. 2009a;364(1):48–56. doi:10.1016/j.apcata.2009.05.022.

Izadbakhsh A, Farhadi F, Khorasheh F, et al. Key parameters in hydrothermal synthesis and characterization of low silicon content SAPO-34 molecular sieve. Microporous Mesoporous Mater. 2009b;126(1–2):1–7. doi:10.1016/j.micromeso.2008.12.009.

Lee YJ, Baek SC, Jun KW. Methanol conversion on SAPO-34 catalysts prepared by mixed template method. Appl Catal A Gen. 2007;329(10):130–6. doi:10.1016/j.apcata.2007.06.034.

Lei W, Liu Z, Lin X, et al. Effect of SAPO-34 molecular sieve morphology on methanol to olefins performance. Chin J Catal. 2013;34(7):1348–56. doi:10.1016/S1872-2067(12)60575-0.

Li J, Li Z, Han D, et al. Facile synthesis of SAPO-34 with small crystal size for conversion of methanol to olefins. Powder Technol. 2014;262:177–82. doi:10.1016/j.powtec.2014.04.0820032-5910.

Marchi AJ, Froment GF. Catalytic conversion of methanol to light alkenes on SAPO molecular sieves. Appl Catal. 1991;71(1): 139–52. doi:10.1016/j.apcata.2007.06.034.

Matsukata M, Ogura M, Osaki T, et al. Conversion of dry gel to microporous crystals in gas phase. Top Catal. 1999;9(1):77–92. doi:10.1023/A:1019106421183.

Pastore HO, Coluccia S, Marchese L. Porous aluminophosphates: from molecular sieves to designed acids catalysts. Cheminformatics. 2005;35(44):351–95. doi:10.1002/chin.200544244.

Qi G, Xie Z, Yang W, et al. Behaviors of coke deposition on SAPO-34 catalyst during methanol conversion to light olefins. Fuel Process Technol. 2007;88(5):437–41. doi:10.1016/j.fuproc.2006.11.008.

Qi G, Xie Z, Zhong S, et al. Advances in process research on coal or natural gas to light olefins via methanol. Mod Chem Ind. 2005;. doi:10.16606/j.cnki.issn0253-4320.2005.02.003 (**in Chinese**).

Rao PRHP, Leon CALY, Ueyama K, et al. Synthesis of BEA by dry gel conversion and its characterization. Microporous Mesoporous Mater. 1998;21(4–6):305–13. doi:10.1016/S1387-1811(98)00033-X.

Rao PRHP, Matsukata M. Dry-gel conversion technique for synthesis of zeolite BEA. Chem Commun. 1996;12(12):1441–2. doi:10.1039/CC9960001441.

Roth WJ, Nachtigall P, Morris RE, et al. Two-dimensional zeolites: current status and perspectives. Chem Rev. 2014;114(9): 4807–37. doi:10.1021/cr400600f.

Rothaemel M, Holtmann HD. Methanol to propylene MTP—Lurgi's way. Oil Gas. 2002;28(1):27–30. doi:10.1016/S0167-2991(07)80142-X.

Sastre G, Lewis DW, Catlow CRA. Mechanisms of silicon incorporation in aluminophosphate molecular sieves. J Mol Catal A Chem. 1997;119(1–3):349–56. doi:10.1016/S1381-1169(96)00498-0.

Shen W, Li X, Wei Y, et al. A study of the acidity of SAPO-34 by solid-state NMR spectroscopy. Microporous Mesoporous Mater. 2012;158(8):19–25. doi:10.1016/j.micromeso.2012.03.013.

Simmen A, McCusker LB, Baerlocher C, et al. The structure determination and rietveld refinement of the aluminophosphate AlPO4-18. Zeolites. 1991;11(7):654–61. doi:10.1016/S0144-2449(05)80167-8.

Sun Q, Ma Y, Wang N, et al. High performance nanosheet-like silicoaluminophosphate molecular sieves: synthesis, 3D EDT structural analysis and MTO catalytic studies. J Mater Chem A. 2014;2(42):17828–39. doi:10.1039/C4TA03419H.

Sun Q, Wang N, Bai R, et al. Seeding induced nano-sized hierarchical SAPO-34 zeolites: cost-effective synthesis and superior MTO performance. J Mater Chem A. 2016;4:14978–82. doi:10.1039/c6ta06613e.

Tan J, Liu Z, Bao X, et al. Crystallization and Si incorporation mechanisms of SAPO-34. Microporous Mesoporous Mater. 2002;53(1–3):97–108. doi:10.1016/S1387-1811(02)00329-3.

Tian P, Li B, Xu S, et al. Investigation of the crystallization process of SAPO-35 and Si distribution in the crystals. J Phys Chem C. 2013;117(8):24–9. doi:10.1021/jp311334q.

Tian P, Wei Y, Ye M, et al. Methanol to olefins (MTO): from fundamentals to commercialization. ACS Catal. 2015;5(3): 1922–38. doi:10.1021/acscatal.5b00007.

Wei Y, Li J, Yuan C, et al. Generation of diamondoid hydrocarbons as confined compounds in SAPO-34 catalyst in the conversion of methanol. Chem Commun. 2012;48(25):3082–4. doi:10.1039/c2cc17676a.

Wilson S, Barger P. The characteristics of SAPO-34 which influence the conversion of methanol to light olefins. Microporous Mesoporous Mater. 1999;29(1–2):117–26. doi:10.1016/S1387-1811(98)00325-4.

Xu W, Dong J, Li J, et al. A novel method for the preparation of zeolite ZSM-5. J Chem Soc Chem Commun. 1990;10(10):755–6. doi:10.1039/C39900000755.

Xu L, Du A, Wei Y, et al. Synthesis of SAPO-34 with only Si (4Al) species: effect of Si contents on Si incorporation mechanism and Si coordination environment of SAPO-34. Microporous Mesoporous Mater. 2008;115(3):332–7. doi:10.1016/j.micromeso.2008.02.001.

Yang H, Liu Z, Gao H, et al. Synthesis and catalytic performances of hierarchical SAPO-34 monolith. J Mater Chem. 2010;20(16): 3227–31. doi:10.1039/B924736J.

Yang N, Yue M, Wang Y. Synthesis of zeolites by dry gel conversion. Progress Chem. 2012;24(2):253–61. doi:10.16085/j.issn.1000-6613.2012.3.0253-09 (**in Chinese**).

Ye L, Cao F, Ying W, et al. Effect of different TEAOH/DEA combinations on SAPO-34's synthesis and catalytic performance. J Porous Mater. 2011;18(2):225–32. doi:10.1007/s10934-010-9374-4.

Zhang L, Bates J, Chen D, et al. Investigations of formation of molecular sieve SAPO-34. J Phys Chem C. 2011;115(45): 22309–19. doi:10.1021/jp208560t.

Zhu J, Cui Y, Zeeshan N. In situ synthesis of SAPO-34 zeolites in kaolin microspheres for a fluidized methanol or dimethyl ether to olefins process. Chin J Chem Eng. 2010;18(6):979–87. doi:10.1016/j.cjche.2010.18.6.979-987.